
LATTICE DYNAMICS
AND PHASE TRANSITIONS

Structural Phase Transition in Elpasolite-Like $(\text{NH}_4)_2\text{KWO}_3\text{F}_3$

I. N. Flerov, M. V. Gorev, V. D. Fokina, A. F. Bovina, M. S. Molochev, Yu. V. Boiko,
V. N. Voronov, and A. G. Kocharova

*Kirensky Institute of Physics, Siberian Division, Russian Academy of Sciences,
Akademgorodok, Krasnoyarsk, 660036 Russia*

e-mail: flerov@ksc.krasn.ru

Received February 3, 2005

Abstract—A new chemical compound, $(\text{NH}_4)_2\text{KWO}_3\text{F}_3$, was synthesized. The Rietveld-refined crystal structure was found to be cubic at room temperature and to belong to the elpasolite family (space group $Fm\bar{3}m$). The heat capacity and unit cell parameters were studied within a broad temperature range. A second-order phase transition was found to occur at 235.4 K and to be well described in terms of phenomenological theory. Hydrostatic pressure broadens the temperature interval of stability of the cubic phase ($dT_0/dp = -10.8 \text{ K GPa}^{-1}$). A possible model of structural ordering based on a comparison of the entropy parameters and electron density distribution in oxygen and fluorine atoms is discussed.

PACS numbers: 64.70.Kb, 65.40.Ba, 65.40.Gr

DOI: 10.1134/S1063783406010215

1. INTRODUCTION

Chemical compounds with the general formula $A_2A'MO_xF_{6-x}$ (A and A' stand for K, Rb, or Cs; M is Ti, Mo, or W; $x = 1, 3$) have cubic symmetry (space group $Fm\bar{3}m$) in a certain temperature range [1, 2]. In the case of $A = A'$, the compounds have the structure of cryolite (Na_3AlF_6), and, in the case of $A \neq A'$, they have the structure of elpasolite (K_2NaAlF_6), which may become distorted as a result of phase transitions that occur as the temperature decreases [3, 4].

It has recently been found that substitution of the ammonium ion for atomic cations simultaneously in two different crystallographic positions, namely, at an octahedron center ($4b$) and in an interoctahedral void ($8c$), gives rise to a noticeable decrease in the temperature at which the cubic phase of the fluorine–oxygen cryolites $A_3MO_xF_{6-x}$ loses stability [5, 6]. These substitutions cause a pronounced increase in the entropy of the phase transitions, which gives one grounds to consider these transitions to be of distinct order-disorder type. This experimental observation is consistent with the structural models of the cubic phase of some of the $(\text{NH}_4)_3MO_xF_{6-x}$ compounds analyzed in [5]. It turned out that the presence of a tetrahedral cation in the structure brings about a substantial increase in the anharmonicity of vibrations of the MO_xF_{6-x} ions, which in the limiting case may become orientationally disordered over four ($96k$), six (mixed $24e + 96j$), or eight ($192l$) equivalent positions.

In the $Fm\bar{3}m$ structure, however, the NH_4 tetrahedra may also act as critical ions [1, 5, 7–10]. In accor-

dance with the environment symmetry, the hydrogen atoms belonging to the NH_4^+ ion at the octahedron center should be distributed over two positions ($32f$ position). On the other hand, the corners of the tetrahedra located both in an interoctahedral void and in the octahedron itself lie on threefold axes; therefore, one cannot rule out the possibility of N–N bond disorder over the three positions ($48f$). A superposition of hydrogen atoms disordered over two and three positions gives rise to the $96k$ position, which is observed, for instance, in $(\text{NH}_4)_3\text{Ti}(\text{O}_2)\text{F}_5$ [11]. Thus, in the presence of complete orientational disorder in the octahedral and tetrahedral subsystems of the cubic phase of ammonium cryolite, a phase transition to a completely ordered phase would be accompanied by a change in entropy of $\Delta S = R(\ln 8 + \ln 2 + \ln 3 + 2\ln 3) = R\ln 432$. It would be difficult, however, to conceive of factors capable of initiating such an extreme amount of disorder. Indeed, calorimetric studies of the fluorine–ammonium cryolites [7–9, 12] have shown that the maximum possible structural disorder corresponds to the octahedra occupying the $192l$ position and to the tetrahedra (in an octahedron) being in position $32f$. In this case, the transition to the ordered (triclinic) phase causes an entropy change of $R(\ln 8 + \ln 2) = R\ln 16$. Replacement of a tetrahedral cation in position $4b$ with a spherical cation initiates ordering of the octahedra in the cubic phase of elpasolite, while at the same time favoring disordering of tetrahedra in interoctahedral voids [13]. It turned out that this entails a completely different pattern of structural distortions induced by phase transitions. For instance, the transition to the tetrahedral phase in the subsystem of octahedra in $(\text{NH}_4)_2\text{KGaF}_6$ is realized as

a displacive type and a further lowering of temperature brings about ordering of the tetrahedra as a result of a second phase transition.

Structural data have seemed to suggest [5] that, in ammonium oxyfluorides with cryolite structure, one could expect a structural ordering similar to that observed in fluorides [7–9, 12]. It turned out, however, that, at atmospheric pressure and temperatures down to 80 K, the phase transitions in $(\text{NH}_4)_3\text{MO}_x\text{F}_{6-x}$ (M stands for Ti or W; $x = 1, 3$) are accompanied by a substantially smaller entropy change ($\Delta S = R \ln 8$) [6]. One may thus expect that substitution of some elements in the oxyfluoride structure may give rise to effects different from those observed in fluorine cryolite–elposolites.

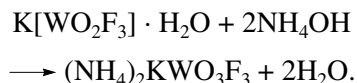
We report on a study of the effect of the transformation of the cryolite structure into an elposolite structure on the properties of cubic oxyfluoride crystals with $Fm\bar{3}m$ symmetry. A new chemical compound, $(\text{NH}_4)_2\text{KWO}_3\text{F}_3$, was prepared, and its structural and calorimetric characteristics were established, in particular, at hydrostatic pressures. The purpose of our work included determination of the structure of the original phase, a search for and characterization of possible phase transitions, and identification of the critical ions responsible for their realization.

2. PREPARATION OF SAMPLES AND THE SEARCH FOR PHASE TRANSITIONS

Samples of $(\text{NH}_4)_2\text{KWO}_3\text{F}_3$ in powder form were prepared by two methods, namely, from solutions and in solid-phase reactions.

The solid-phase synthesis was performed in an autoclave with a Teflon insert in a vertical tube furnace providing a constant axial temperature gradient of $\sim 20 \text{ K cm}^{-1}$. The reaction was conducted at 570 K over a period of a week. The starting components were calcined WO_3 and $(\text{NH}_4)\text{F}$, as well as KF prepared by oriented crystallization from a KF-HF melt in a platinum boat. The reagents were taken in stoichiometric ratio.

The preparation of $(\text{NH}_4)_2\text{KWO}_3\text{F}_3$ from a solution was carried out in three stages. In the first stage, an aqueous solution of K_2WO_4 was saturated with hydrofluoric acid to $pH \sim 3-4$. This procedure yielded $\text{K}_2[\text{WO}_2\text{F}_4] \cdot \text{H}_2\text{O}$ in 20 h. This compound was subsequently dissolved in hydrofluoric acid, and the solution was left to evaporate at room temperature for 20–30 h to produce $\text{K}[\text{WO}_2\text{F}_3] \cdot \text{H}_2\text{O}$ crystals. Finally, $(\text{NH}_4)_2\text{KWO}_3\text{F}_3$ was synthesized in the reaction



Characterization of the samples thus prepared was effected by plasma photometry on a FLAPHO 4 instrument and showed the potassium content to correspond

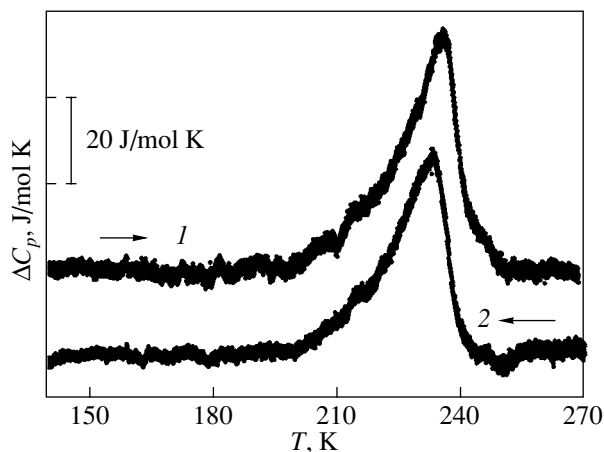


Fig. 1. Temperature dependence of the anomalous heat capacity associated with a phase transition in $(\text{NH}_4)_2\text{KWO}_3\text{F}_3$ measured by DSM in (1) the heating and (2) cooling modes.

to the chemical formula $(\text{NH}_4)_2\text{KWO}_3\text{F}_3$. X-ray diffraction performed on a DRON-2 setup established that $(\text{NH}_4)_2\text{KWO}_3\text{F}_3$ crystals at room temperature are cubic ($Fm\bar{3}m$, $Z = 4$), which is characteristic of crystals with an elposolite structure. No reflections indicative of foreign phases were detected in the diffraction pattern. Substitution of the spherical potassium ion for the tetrahedral ammonium cation resulted, as expected, in a considerable decrease of the cell parameter in size ($a_0 = 0.8958 \text{ nm}$) as compared to the cryolite $(\text{NH}_4)_3\text{WO}_3\text{F}_3$ ($a_0 = 0.9156 \text{ nm}$) [6].

The search for phase transitions in $(\text{NH}_4)_2\text{KWO}_3\text{F}_3$ was performed by studying the temperature dependences of its heat capacity and unit cell parameters with the use of differential scanning microcalorimetry (DSM) and x-ray powder diffractometry.

The heat capacity of samples prepared by the two methods was measured with a DSM-2M instrument in the 110- to 330-K temperature interval under heating and cooling at a rate of $\pm 8 \text{ K/min}$. The sample mass was 0.15–0.25 g. The heat capacity revealed an anomalous behavior, which was reproducible under thermal cycling and implied the existence of a phase transition in this compound at a temperature $T_0 = 235 \pm 2 \text{ K}$ (Fig. 1). Multiple measurements yielded for the corresponding enthalpy change $\Delta H_0 = 1100 \pm 150 \text{ J/mol}$.

The DSM data on T_0 and ΔH_0 obtained on samples prepared by different methods agree with one another within measurement error.

The occurrence of a structural phase transition in $(\text{NH}_4)_2\text{KWO}_3\text{F}_3$ was corroborated by x-ray powder diffraction measurements made on a DRON-2 setup within a broad temperature interval. The formation of a low-symmetry phase at $T < T_0$ manifested itself in a broadening and splitting of the $(h00)$ and $(hk0)$ reflec-

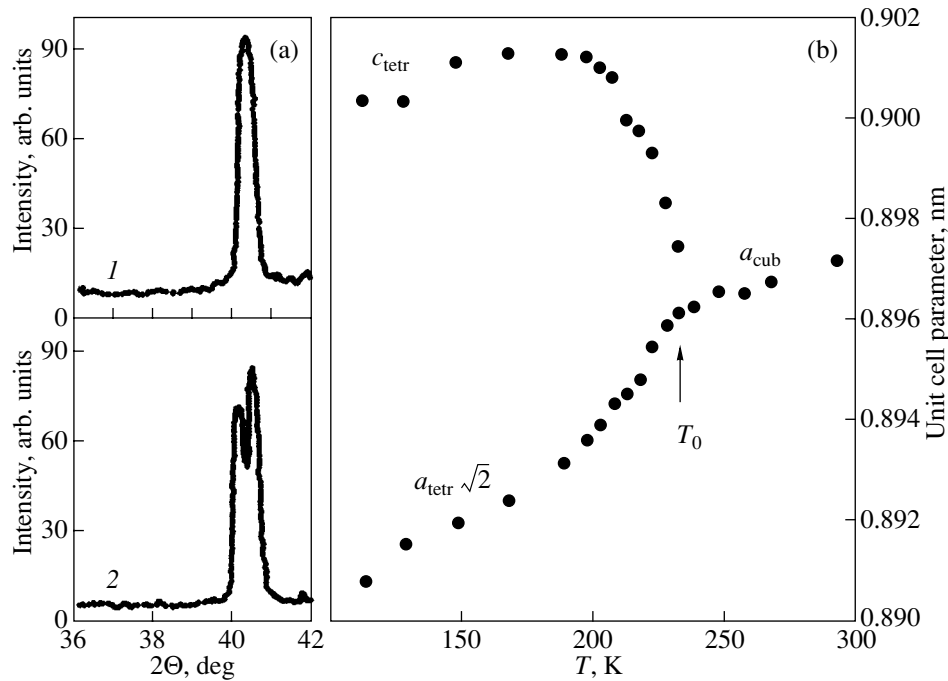


Fig. 2. X-ray studies of $(\text{NH}_4)_2\text{KWO}_3\text{F}_3$: (a) the (400) reflection obtained at (1) 293 and (2) 123 K and (b) the temperature dependence of the unit cell parameters.

tions. Figure 2a shows a characteristic pattern of the (400) reflection for the cubic and distorted phases.

We succeeded in indexing most of the lines in the x-ray diffraction pattern of $(\text{NH}_4)_2\text{KWO}_3\text{F}_3$ in the pseudotetragonal-cell approximation. The temperature dependence of the unit cell parameters, $a_i(T)$, is presented in Fig. 2b. No sharp change in the parameters occurs at the transition point, which argues for a second-order phase transformation. This conclusion is borne out by the absence of any hysteresis in the tem-

perature of the phase transition detected in DSM studies of the heat capacity of this compound.

3. CALORIMETRIC MEASUREMENTS AND THE PHASE DIAGRAM

To refine the thermodynamic parameters of the phase transition, we carried out a detailed study of the temperature dependence of the heat capacity of $(\text{NH}_4)_2\text{KWO}_3\text{F}_3$ using adiabatic calorimetry in the 80- to 300-K temperature interval.

A sample 1.766 g in mass was placed in an air-tight indium container in a helium atmosphere. Measurements were performed in the discrete ($\Delta T = 2.5\text{--}4.0$ K) and continuous ($dT/dt = 0.14$ K/min) heating modes. The temperature was measured with a platinum resistance thermometer.

Figure 3a plots the temperature dependence of the heat capacity of the elpasolite-like $(\text{NH}_4)_2\text{KWO}_3\text{F}_3$. One heat capacity anomaly is observed, as in the DSM studies. The averaged phase transition temperature was found to be $T_0 = 235.4 \pm 0.1$ K. The dashed line in Fig. 3a shows the lattice heat capacity C_L , which was isolated by polynomial approximation of the $C_p(T)$ experimental data outside the region of the heat capacity anomaly. The excess heat capacity ΔC_p was determined by subtracting the lattice contribution from the total heat capacity. At the phase transition point, the $\Delta C_p/C_L$ ratio is small (25%), which bears out the sug-

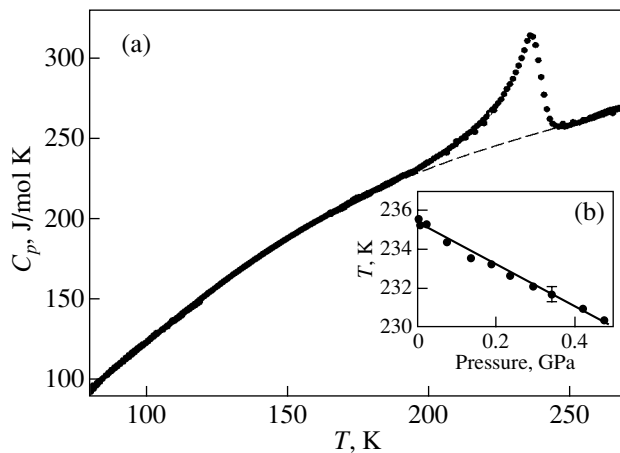


Fig. 3. (a) Temperature dependence of the heat capacity within a broad temperature interval and (b) the T - p phase diagram of oxyfluoride $(\text{NH}_4)_2\text{KWO}_3\text{F}_3$.

gestion that $(\text{NH}_4)_2\text{KWO}_3\text{F}_3$ undergoes a second-order phase transition.

The change in enthalpy due to the structural transformation, derived by integrating the $\Delta C_p(T)$ function in the 170- to 250-K interval, was found to be $\Delta H_0 = 1060 \pm 60 \text{ J/mol}$.

Earlier studies of the related, cryolite-like $(\text{NH}_4)_3\text{WO}_3\text{F}_3$, which also has the cubic structure $Fm\bar{3}m$ at room temperature and undergoes a sequence of two phase transitions within a narrow temperature interval, showed this compound to be very sensitive to hydrostatic pressure [6]. A triple point was found in the T - p phase diagram of the oxyfluoride $(\text{NH}_4)_3\text{WO}_3\text{F}_3$ already at a pressure of $\sim 0.18 \text{ GPa}$.

To investigate the effect of pressure on the stability of the cubic phase of $(\text{NH}_4)_2\text{KWO}_3\text{F}_3$, we carried out calorimetric studies by differential thermal analysis (DTA). The experimental technique employed to measure the $T(p)$ dependence was similar to that used in [6]. Figure 3b shows the results of the study of the T - p phase diagram. The region within which the cubic phase exists was established to broaden with increasing pressure. The pressure coefficient of the phase transition temperature is $dT_0/dp = -10.8 \pm 0.8 \text{ K GPa}^{-1}$. No triple points or pressure-induced phases were detected up to 0.5 GPa.

4. STRUCTURAL STUDIES

The Rietveld procedure was used to refine the structure of the $(\text{NH}_4)_2\text{KWO}_3\text{F}_3$ cubic phase. For this purpose, we analyzed the x-ray diffraction spectra of polycrystalline samples obtained on a D8-ADVANCE x-ray diffractometer ($\text{CuK}\alpha$ radiation, θ - 2θ scanning). The scanning step in the angle 2θ was 0.02° with a 15-s exposure at each point. To reduce the effect of texture on the reflection intensity, the samples were rotated at a rate of 0.5 s^{-1} .

Our subsequent plans included an analysis of the totality of experimental data in order to reveal the influence of the isovalent substitution $(\text{NH}_4)^+ \rightarrow \text{K}^+$ on the properties and structure of oxyfluorides. Therefore, in addition to polycrystalline $(\text{NH}_4)_2\text{KWO}_3\text{F}_3$, we also performed structural studies on $(\text{NH}_4)_3\text{WO}_3\text{F}_3$, although the structure of the latter compound had already been refined in [5].

The experimental data arrays were treated using the WTREOR [14] and WINPLOTR [15] codes. A Voigt function was chosen to describe the peak shape. The refinement of the structure was effected with fixed coordinates of hydrogen and nitrogen atoms. Taking into account the hydrogen atoms brought about a decrease in the reliability factor R . The thermal parameters of the H and N atoms likewise were not refined, because this procedure yielded negative values. The position populations of these atoms were not refined.

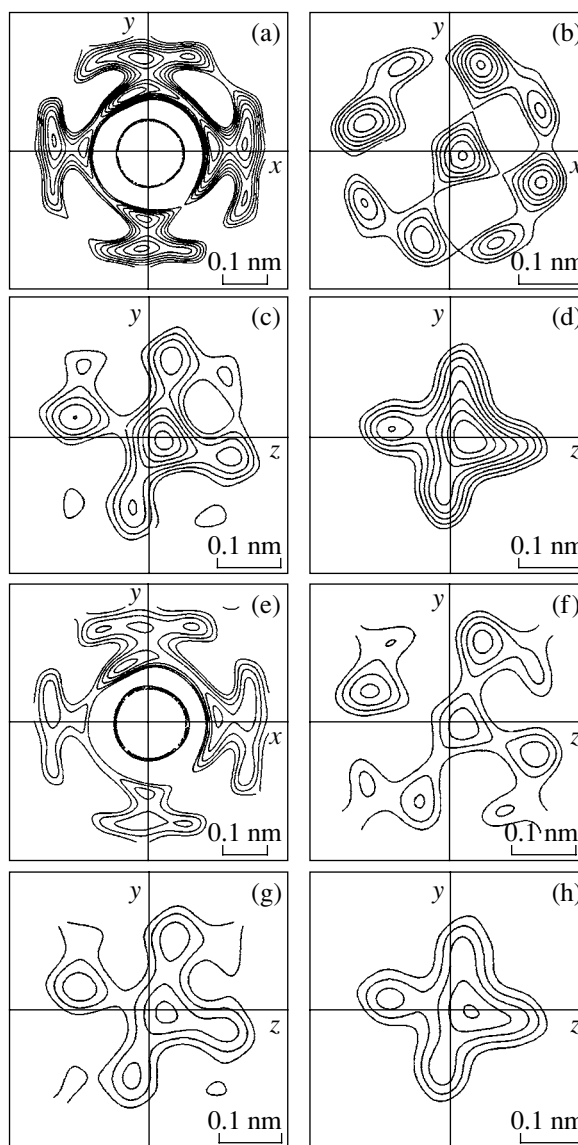


Fig. 4. Electron density maps (400 e/nm^3 step) calculated for (a-d) $(\text{NH}_4)_2\text{KWO}_3\text{F}_3$ and (e, f) $(\text{NH}_4)_3\text{WO}_3\text{F}_3$ at (a, e) $z = 0$ and x equal to (b, f) 0.195, (c, g) 0.215, and (d, h) 0.235.

The initial structural model of both compounds was specified by setting the coordinates of atoms of the starting compound $(\text{NH}_4)_3\text{WO}_3\text{F}_3$ found in [5]. The O and F atoms were in position $24e (x; 0; 0)$ with an occupancy of 0.5. The refinement of their x coordinates yielded $-0.2165(5)$ and $-0.2144(6)$ for $(\text{NH}_4)_2\text{KWO}_3\text{F}_3$ and $(\text{NH}_4)_3\text{WO}_3\text{F}_3$, respectively. The thermal parameters of the W and K atoms were refined using the isotropic model.

The results of these studies were used to construct electron density maps (Fig. 4). The pronounced asymmetry in the density distribution pattern relative to the axes may be accounted for by anomalous x-ray absorp-

Table 1. Data retrieval and structure refinement parameters

Characteristic	(NH ₄) ₂ KWO ₃ F ₃	(NH ₄) ₃ WO ₃ F ₃
Space group	$Fm\bar{3}m$	$Fm\bar{3}m$
a_0 , nm	0.89585 (8)	0.91527 (2)
V , nm ³	0.71897 (1)	0.76674 (2)
2 θ angle interval, deg	15.00–111.00	14.00–110.00
Number of Bragg reflections	40	40
Number of refined parameters	5	4
R_p , %	11.1	11.9
R_{wp} , %	13.1	14.1
R_B , %	5.03	5.2

Note: a_0 is the unit cell parameter, and V is the unit cell volume; R_p , R_{wp} , and R_B are the profile, weighted profile, and Bragg reliability factors, respectively.

Table 2. Atomic coordinates, isotropic thermal parameters (B_{iso}), and position occupancy (p)

Atom	p	x	y	z	$B_{iso} \times 10^2$ nm ²
(NH ₄) ₂ KWO ₃ F ₃					
W	1.0	0	0	0	1.83 (2)
K	1.0	0.5	0.5	0.5	1.53 (7)
N	1.0	0.25	0.25	0.25	1.0
H	1.0	0.198	0.198	0.198	1.0
F	0.5	-0.2165 (5)	0	0	2.69*
O	0.5	-0.2165 (5)	0	0	2.69*
(NH ₄) ₃ WO ₃ F ₃					
W	1.0	0	0	0	1.43 (8)
N (1)	1.0	0.25	0.25	0.25	1.0
H (1)	1.0	0.198	0.198	0.198	1.0
N (2)	1.0	0.5	0.5	0.5	1.0
H (2)	0.5	0.558	0.558	0.558	1.0
F	0.5	-0.2144 (6)	0	0	6.5*
O	0.5	-0.2144 (6)	0	0	6.5*

* Thermal parameter of an anisotropic model.

Table 3. Thermodynamic parameters of the phase transitions in accordance with Eqs. (1) and (2) for the (NH₄)₂KWO₃F₃ and (NH₄)₃WO₃F₃ compounds

Compound	A_T^2/B , J/mol K ²	A_T^3/C , J ² /mol ² K ³	N
(NH ₄) ₂ KWO ₃ F	0.615	2.64	0.099
(NH ₄) ₃ WO ₃ F ₃	0.32	1.84	0.175

tion by tungsten atoms. At $z = 0$, the ellipsoid of fluorine and oxygen thermal vibrations for both compounds is a strongly distorted ellipsoid of revolution with one of the radii close to zero (Figs. 4a, 4e). Thus, the electron density distribution pattern indicates that the thermal parameters of the O and F atoms should be refined in an anisotropic approximation. This procedure yielded the following parameters: $U_{11} = 0.5 \times 10^{-4}$ nm² and $U_{22} = U_{33} = 1.01(7) \times 10^{-4}$ nm² for (NH₄)₂KWO₃F₃ and $U_{11} = 0.5 \times 10^{-4}$ nm² and $U_{22} = U_{33} = 3.1(7) \times 10^{-4}$ nm² for (NH₄)₃WO₃F₃. Final results on the refined structure of both compounds are presented in Table 1, and the atomic coordinates, isotropic thermal parameters, and position occupancies are listed in Table 2.

5. DISCUSSION OF THE RESULTS

Thus, our calorimetric, x-ray, and DTA studies of crystalline (NH₄)₂KWO₃F₃ under pressure revealed that replacement of a tetrahedral cation in the 4b position with a spherical cation gives rise to the following effects.

The cubic $Fm\bar{3}m$ phase persists at room temperature. The temperature at which it loses stability rises by ~35 K.

The phase transition from the cubic phase changes from first-order (in (NH₄)₃WO₃F₃) to second-order (in (NH₄)₂KWO₃F₃). The $\Delta C_p/C_L$ ratio, as shown both in the present study and in [6], is ~25% in both compounds. Also, excess heat capacity persists within a fairly broad temperature region.

It appears of interest to analyze the temperature dependence of the anomalous heat capacity of both compounds associated with structural transformations in terms of the Landau thermodynamic theory. According to [16], the quantity $(\Delta C_p/T)^{-2}$ below the transition point is a linear function of temperature:

$$\left(\frac{\Delta C_p}{T}\right)^{-2} = \left(\frac{2\sqrt{B^2 - 3A'C}}{A_T^2}\right)^2 + \frac{12C}{A_T^3}(T_0 - T). \quad (1)$$

Here, $A = A' + A_T(T - T_0)$, B , and C are coefficients of the thermodynamic potential $\Delta\Phi(p, T, \eta) = A\eta^2 + B\eta^4 + C\eta^6$.

The temperature dependences of the inverse square of the excess heat capacity are presented graphically in Fig. 5. Relation (1) for both tungsten compounds is seen to be satisfied in the temperature interval $\sim(T_0 - 8$ K). The behavior of the heat capacity of (NH₄)₃WO₃F₃ undergoing two successive first-order phase transitions within an interval as narrow as ~1.5 K was analyzed with respect to the heat capacity at the low-temperature transition point T_2 .

Table 3 lists the ratios of the coefficients of Eq. (1) and the quantity N characterizing the extent to which

the transitions approach the tricritical point [16]:

$$N = \sqrt{\frac{B^2}{3A_7CT_C}}. \quad (2)$$

Here, $T_C = T_0 - B^2/(4A_7C)$ is the Curie temperature.

The data obtained in the present study on the heat capacity of elpasolite-like $(\text{NH}_4)_2\text{KWO}_3\text{F}_3$ were used to calculate the phase transition entropy $\Delta S_0 = 4.7 \pm 0.3 \text{ J/mol K}$. The course of its variation with temperature can be derived from Fig. 6, which also presents for comparison the temperature dependence of $\Delta S/T$ for cryolite-like $(\text{NH}_4)_3\text{WO}_3\text{F}_3$ [6]. We readily see that the above cation substitution gave rise to a noticeable decrease in entropy. A possible explanation for this is that the $(\text{NH}_4)_2\text{KWO}_3\text{F}_3$ structure in the starting phase is more ordered or that the transition observed to occur in this compound results in only partial ordering of the critical ions. In the latter case, one might suggest that, at lower temperatures ($T < 80 \text{ K}$), the elpasolite-like compound under study undergoes an additional phase transition.

The tetrahedral cation occupying position $4b$ in an $Fm\bar{3}m$ lattice is distributed over two positions from symmetry considerations. Its replacement with a spherical cation should substantially reduce the amount of disorder in the structure. This pattern was indeed observed in the related fluorides $(\text{NH}_4)_3\text{GaF}_6 \rightarrow (\text{NH}_4)_2\text{KGaF}_6$ [13]; namely, the order–disorder transition in the cryolite-like compound (with $\Delta S = R\ln 16$) transformed to the displacive type (with $\Delta S \approx 0.1R$) as a result of cation substitution.

The entropy of the phase transition in $(\text{NH}_4)_2\text{KWO}_3\text{F}_3$ ($\sim R\ln 1.76$) far exceeds the value characteristic of displacive-type transitions and is close to $\Delta S_1 = R\ln 1.68$, a value typical of cryolite-like $\text{K}_3\text{WO}_3\text{F}_3$ [3], which undergoes a sequence of two phase transitions. We believe that the above observations argue both for a really strong effect of the size and shape of a cation in position $4b$ on the transition mechanism and for the validity of the assumption that the structure of elpasolite-like $(\text{NH}_4)_2\text{KWO}_3\text{F}_3$ can disorder still further.

The question regarding the character of disorder of at least the octahedral ions can be answered by mapping the electron density, whose cross sections for the tungsten oxyfluorides are shown in Fig. 4. The electron density contours of both compounds at various distances of the cross sections from the octahedron center are practically identical. However, the concentration of isolines corresponding to the coordinate of the oxygen (fluorine) atom in position $24e$ ($x = 0.215$) is higher for $(\text{NH}_4)_2\text{KWO}_3\text{F}_3$. All this implies that the oxygen–fluorine octahedra in the cubic phase of both oxyfluorides are disordered but that in the potassium compound the amount of their disorder is smaller.

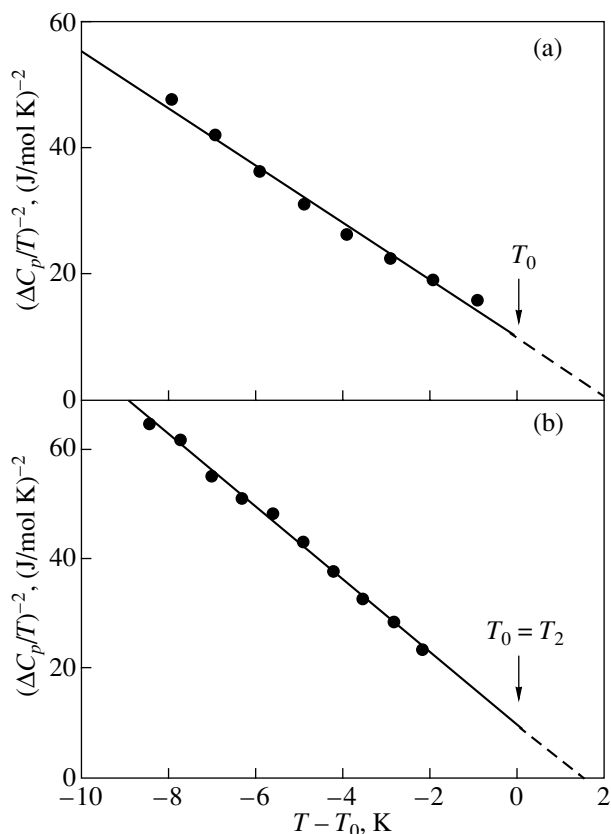


Fig. 5. Temperature dependences of the inverse square of the excess heat capacity for (a) $(\text{NH}_4)_2\text{KWO}_3\text{F}_3$ and (b) $(\text{NH}_4)_3\text{WO}_3\text{F}_3$.

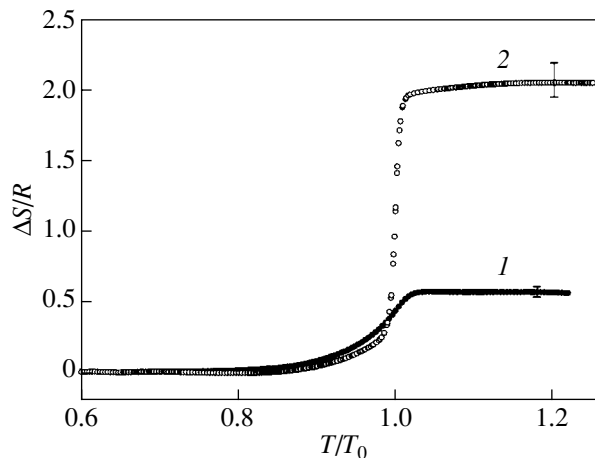


Fig. 6. Temperature dependences of the entropy of the phase transitions occurring in (1) $(\text{NH}_4)_2\text{KWO}_3\text{F}_3$ and (2) $(\text{NH}_4)_3\text{WO}_3\text{F}_3$ [6]; R is the universal gas constant.

In order to gain a more detailed understanding of the mechanism of the phase transition in $(\text{NH}_4)_2\text{KWO}_3\text{F}_3$, one should, in our opinion, perform calorimetric studies below 80 K , determine the symmetry, and refine the structure of the distorted phase.

ACKNOWLEDGMENTS

This study was supported by the Russian Foundation for Basic Research (project no. 03-02-16079), the Foundation for Support of National Science, the Krasnoyarsk Krai Science Foundation (project no. 14G110), and a program of the Department of Physical Sciences of the Russian Academy of Sciences (project no. 2.6).

REFERENCES

1. I. N. Flerov, M. V. Gorev, K. S. Aleksandrov, A. Tressaud, J. Grannec, and M. Couzi, *Mater. Sci. Eng., R* **24** (3), 81 (1998).
2. Von G. Pausewang and W. Rüdorff, *Z. Anorg. Allg. Chem.* **364** (1–2), 69 (1969).
3. G. Peraudeau, J. Ravez, P. Hagenmüller, and H. Arend, *Solid State Commun.* **27**, 591 (1978).
4. M. Fouad, J. P. Chaminade, J. Ravez, and P. Hagenmüller, *Rev. Chim. Min.* **24**, 1 (1987).
5. A. A. Udovenko, N. M. Laptash, and I. G. Maslennikova, *J. Fluorine Chem.* **124**, 5 (1999).
6. I. N. Flerov, M. V. Gorev, V. D. Fokina, A. F. Bovina, and N. M. Laptash, *Fiz. Tverd. Tela (St. Petersburg)* **46** (5), 888 (2004) [*Phys. Solid State* **46** (5), 915 (2004)].
7. K. Moriya, T. Matsuo, H. Suga, and S. Seki, *Bull. Chem. Soc. Jpn.* **50** (8), 1920 (1977).
8. K. Moriya, T. Matsuo, H. Suga, and S. Seki, *Bull. Chem. Soc. Jpn.* **52** (11), 1352 (1979).
9. A. Tressaud, S. Khairoun, L. Rabardel, T. Kobayashi, T. Matsuo, and H. Suga, *Phys. Status Solidi A* **96** (2), 407 (1986).
10. K. Hirokawa and Y. Furukawa, *J. Phys. Chem. Solids* **49** (9), 1047 (1988).
11. W. Massa and G. Pausewang, *Mater. Res. Bull.* **13**, 361 (1978).
12. I. N. Flerov, M. V. Gorev, and T. V. Ushakova, *Fiz. Tverd. Tela (St. Petersburg)* **41** (3), 523 (1999) [*Phys. Solid State* **41** (3), 468 (1999)].
13. I. N. Flerov, M. V. Gorev, M. L. Afanas'ev, and T. V. Ushakova, *Fiz. Tverd. Tela* **43** (12), 2204 (2001) [*Phys. Solid State* **43** (12), 2301 (2001)].
14. P.-E. Werner, L. Eriksson, and M. Westdahl, *J. Appl. Crystallogr.* **18**, 367 (1985).
15. T. Roisnel and J. Rodrigues-Carvajal, in *Proceedings of the 7th European Powder Diffraction Conference, Barcelona, Spain, 2000, Parts 1–2 (EPDIC-7)* **378/381**, 118 (2001).
16. K. S. Aleksandrov and I. N. Flerov, *Fiz. Tverd. Tela (Leningrad)* **21** (2), 327 (1979) [*Sov. Phys. Solid State* **21** (2), 195 (1979)].

Translated by G. Skrebtsov